

Available online at www.sciencedirect.com**ScienceDirect**

Procedia Chemistry 14 (2015) 56 – 65

Procedia
Chemistry

2nd Humboldt Kolleg in conjunction with International Conference on Natural Sciences,
HK-ICONS 2014

Hydrothermal Carbonation of K–Rich Ash, Value Added Energy Engineering and CO₂ Mineral Sequestration

Anggoro Tri Mursito^{a*}, Anita Yuliyanti^a, Jakah^a

^aResearch Centre for Geotechnology, Indonesian Institute of Sciences (LIPI), Jl. Sangkuriang, Gd. 70, Bandung 40135, Indonesia

Abstract

In this paper, hydrothermal carbonation of raw K–rich ash derived from a palm oil plant factory in West Kalimantan, Indonesia had been studied and evaluated at varying temperatures of 50 °C to 300 °C, initial CO₂ pressure at between 2 MPa to 2.5 MPa and a maximum final pressure of 8.5 MPa and a residence time of 30 min. The yield of the solid products was about between 47 wt% and 66 wt% and the effective CO₂ content which was captured by hydrothermally solid products was between 0.057 ton · ton^{−1} and 0.115 ton · ton^{−1} following hydrothermal carbonation. In addition, dehydration of solid product occurred at mostly 300 °C, while oxidation was started at 50 °C. Obviously, both the sorption–dissociation of CO₂ in the solution and hydrothermal carbonation process produce a global pressure drop in the system resulting in CO₂ mineral sequestration. The carbonation efficiency of solid–fluid interactions at 25 °C and after 24 h period was 25.36 % and 0.05 954 mol of CO₂ were consumed by the carbonation process. At the condition applied, observed several possibilities were observed such as: the pH (alkalinity), total inorganic carbon, direct precipitation of carbonates minerals as well as crystallization of carbonates in the solution and solid products.

© 2015 Published by Elsevier B.V. This is an open access article under the CC BY-NC-ND license (<http://creativecommons.org/licenses/by-nc-nd/4.0/>).

Peer-review under responsibility of the Scientific Committee of HK-ICONS 2014

Keywords: Carbonation; CO₂ captured and storage; CO₂ mineral sequestration; hydrothermal treatment; K-rich ash

* Corresponding author. Tel.: +62 816 426 3818; Fax: +62 22 250 4593
E-mail address: anggoro@geotek.lipi.go.id

Nomenclature

Al	aluminium	L	liter
Ca	calcium	Mg	magnesium
CaO	calcium oxide	min	minute
Ca(OH)₂	calcium hydroxide	MPa	mega pascal
CDM	Clean Development Mechanism, a Kyoto Protocol mechanism to assist developing countries reducing their greenhouse gas emissions	wt%	percent weight
		ton	10 ³ kg
		h	hour
CE	carbonation efficiency	pH	is a measure of the acidity or basicity of an aqueous solution
CO₂	carbon dioxide	MW	mega watt
FTIR	fourier transform infrared	rpm	revolutions per minute, is a measure of the frequency of a rotation (1/60 Hz).
g	gram	Si	silicon
GHG	greenhouse gas	SiO₂	silicon dioxide
Gt	giga ton	TIC	total inorganic carbon
HCO₃⁻	bicarbonate/hydrogen carbonate	TOC	total organic carbon
K	kalium/potassium	UP	ultra pure
K₂O	potassium oxide	XRF	X-ray fluorescence
Ksp	solubility product constant	XRD	X-ray diffraction

1. Introduction

The consumption of coal for electricity generation is 39.7×10^6 ton of 25 power plants in 2008, with 11 376MW of installed capacity in Indonesia. The use of coal releases proportionately more CO₂ emission than other fossil energy carriers (oil and gas). Indonesian peatland fires are predominantly anthropogenic and source of more CO₂ emission, started by local (indigenous) and immigrant farmers as part of small-scale land clearance activities, and also, on a much larger scale, by private companies and government agencies as the principal method of clearing forest before crops are established. Total CO₂ emissions from Indonesia alone have increased about 38 % from 233.0 in 1998 to 376.3×10^6 ton in 2008 and are projected to increase in the future¹. This was only one-fourth of total CO₂ emission of Japan in 2008 which was 1390.6×10^6 ton. Page et al estimated that between 0.81 and 2.57 Gt of carbon were released into the atmosphere in 1997 from Indonesia as a whole, as the result of burning peat and vegetation². This CO₂ emission will continuously increase with the construction of new coal fired power plant and the increase on the capacity of existing coal fired power plant.

Several evidences of man-made climate change have been accumulating over the past decades. Rising carbon dioxide concentrations due to anthropogenic emissions are scientifically proven to be the main cause for it. One of the alternatives to reduce the CO₂ emission without modifying and/or combined within the energy production system is the retention or sequestration of carbon dioxide in stable geological reservoirs³⁻⁶. Moreover, the CO₂ dissolution into the pore water and the consequent carbonic acid formation can result in the dissolution of several minerals (mainly carbonate, oxides and hydroxide minerals) affecting the long-term confinement properties of the reservoirs⁷. Although this mechanism favors the permanent CO₂ sequestration, it is expected to be slow in geological formation (hundreds of years) due to the slow kinetics of silicate mineral dissolution and carbonate mineral precipitation.

Various publications⁸⁻¹³ have proposed the mineral sequestration of CO₂ in controlled reactors as a viable approach to reduce CO₂ emissions into the atmosphere using liquid or solid alkaline residues such as municipal-waste combustion fly-ash, bottom ash, brine alkaline solutions, waste concrete and cements, steel slag, coal combustion fly-ash, alkaline paper mill waste, asbestos, etc. In 1896, a Swedish chemist put forward the idea that

CO₂ emissions from the combustion of coal could enhance the greenhouse effect; leading to adverse catastrophic consequences caused by global warming¹⁴ and has been proved¹⁵. At present, Indonesia is not subjected to any commitments towards reducing GHG emissions. However, as Parties to Kyoto, Indonesia can voluntarily participate in the CDM and benefit from investments in the GHG emission reduction projects¹⁶.

The objective of the research was to utilize and demonstrate that K-rich ash could be used for the CO₂ sequestered material treated by hydrothermal carbonation. Specific purpose of this research is to estimate the dissolution rate of CO₂ for each experiment as well as to study the kinetic of carbonates precipitation and to understand the carbonation capacity and its mechanism.

2. Material and methods

Raw K-rich ash samples were obtained from a palm oil plant factory in West Kalimantan, Indonesia. The experiments were conducted in a 0.5 L batch-type reactor which has been described elsewhere^{17–19}. The amount of the slurry added to the reactor was 300 g, corresponding to 50 g of moisture-free K-rich ash. The reactor was then pressurized with high purity CO₂ to 1.0 MPa, 2.0 MPa and 2.5 MPa at ambient temperature. Next, the raw peat was heated with agitation at 200 rpm while the reaction temperature was automatically adjusted from 50 °C to 300 °C at an average heating rate of 6.6 °C · min⁻¹. After the desired reaction time of 30 min, the reactor was cooled immediately. After cooling down, the gas products were released through a gasometer and the volume was calculated manually. The solid and liquid phases were then collected from the reactor and separated by filtration using a water aspirator. The liquid product was analyzed for total inorganic carbon (TIC) using a TOC analyzer. The solid products were analyzed by Fourier transform infrared spectroscopy (FTIR), X-ray fluorescence (XRF) and X-ray diffraction (XRD). The photomicrograph and petrography of solid product were analyzed for optical properties and mineral identification by using binocular polarizing microscope.

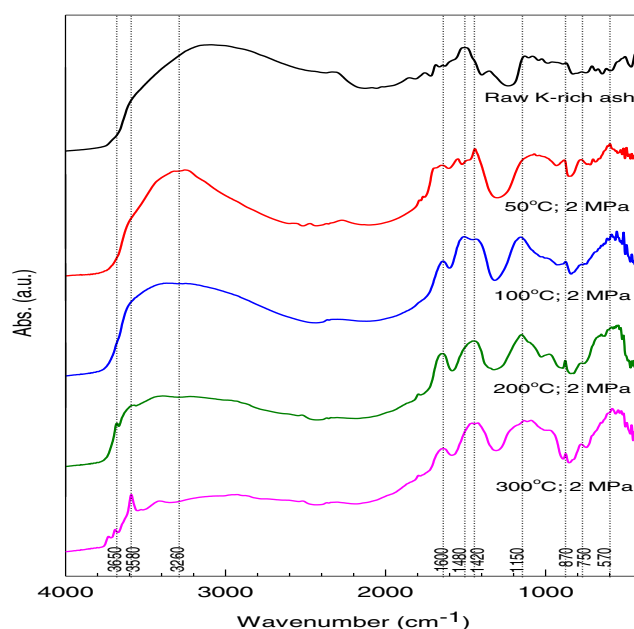
3. Results and discussion

Table 1 shows the concentration of oxide elements of raw K-rich ash and solid products treated at different CO₂ pressures and temperature as being measured by XRF. Raw K-rich ash contained for about 70 wt% of K₂O followed by Si, Ca, Al and Mg oxides. This ash is rich in alkaline earth elements was possibly contained in palm oil trees and the nutrients from earth or land. Empty fruit bunch has an averagely high ash content for more than 3 wt%, eventhough other wastes generated from palm oil trees such as fiber, shell, trunk and frond has lower K₂O content. As increasing treated temperature and CO₂ treated pressure, CaO and SiO₂ content of solid product increased manifold. While K₂O content in solid products decreased due to the high solubility in water. These indicated that possibly Ca containing carbonates were decomposed and remained in solid products as well as Si.

Development of the carbonation process that affects on oxygen functional explained by using FTIR spectroscopy analysis. Determinations of the peaks in each spectrum of the main functional groups were obtained from several publications^{18, 20–21}. Fig. 1 explains about the development of oxygen and other functional group analysis results of raw K-rich ash and solid products. The examination of the (3 500 to 3 100) cm⁻¹ zone revealed a progressive lowering in relative intensity of OH stretch content of the solid products produced started at 30 °C. This peak is somewhat diminished in relative intensity, probably due to the dehydration. The strong bands in the 3 580 cm⁻¹ and 3 650 cm⁻¹ region are due to the Si-OH stretching modes of silicate clay minerals. Increasing relative intensity of Si-OH stretching with increasing treated temperature is clearly seen in the solid product. Increasing relative intensity of C-O stretching in the form of carbonate (CO₃²⁻) at 1 420 cm⁻¹ and 870 cm⁻¹ suggested that carbonation process occurred. In addition, significant changes in the oxygen content of the functional groups can also be observed in the 1 600 cm⁻¹ to 1 100 cm⁻¹ zone. The distribution of increasing of oxygen content of the functional groups was also observed during the process.

Table 1. Metal oxides concentration in raw K-rich ash and solid products

Metal Oxides	Raw (wt%)	Treated at 2.0 MPa (wt%)				Treated at 2.5 MPa (wt%)			
		50 °C	100 °C	200 °C	300 °C	50 °C	100 °C	200 °C	300 °C
K ₂ O	68.195	29.589	24.388	21.155	25.555	31.992	20.199	20.255	22.656
SiO ₂	8.274	22.961	29.621	33.064	36.928	21.801	34.301	33.301	37.444
CaO	8.178	32.599	28.030	28.828	24.677	34.735	31.609	30.330	25.238
Al ₂ O ₃	5.398	0.000	0.000	0.000	0.000	0.000	0.000	0.000	0.000
Cl	4.347	1.346	2.334	1.559	1.286	1.656	1.473	1.635	1.018
MgO	2.029	5.912	7.470	8.137	5.676	5.162	4.898	8.044	7.262
SO ₃	1.279	0.179	0.000	0.207	0.183	0.000	0.233	0.215	0.196
Fe ₂ O ₃	0.000	1.378	1.314	1.610	1.585	0.000	1.914	0.000	1.583

Fig. 1. Typical FTIR spectrum from raw K-rich ash and solid products at selected treated CO₂ pressure (2 MPa)

Decomposition of carbonate and hydration process as a results of hydrothermal carbonation is obviously occurred as shown in Fig. 2. Several spectra belonging to a metal halide salt such as KCl are somehow diminished in relative intensity at all treated temperature especially at high angle. These were possibly due to the high solubility of KCl in water at high temperature. Increasing in a relative intensity of carbonate spectra such as CaCO₃ including the hydrated forms of carbonate such as CaCO₃·H₂O suggested that carbonation and hydration process are simultaneously occurring when the sample contacted with atmospheric CO₂, dissolved CO₂, water and increasing temperature. Both spectra of CaCO₃ and CaCO₃·H₂O increased with increasing CO₂ pressure and temperature. Hydrated forms of CaCO₃·H₂O is diminished in relative intensity at 200 °C and 300 °C treated temperature due the dehydration process. Interestingly, that formed of alkaline hydrated magnesium–silicate (Mg₄Si₆O₁₅(OH)₂·6H₂O) were only formed at treated temperature of 50 °C and 100 °C and at 2 MPa and 2.5 MPa. Other result, related to the formation of SiO₂ which is a major mineralization at high treated temperature and pressure showed to the decomposition of other minerals which are containing K, Mg, Ca partly leached and remained in the solid products.

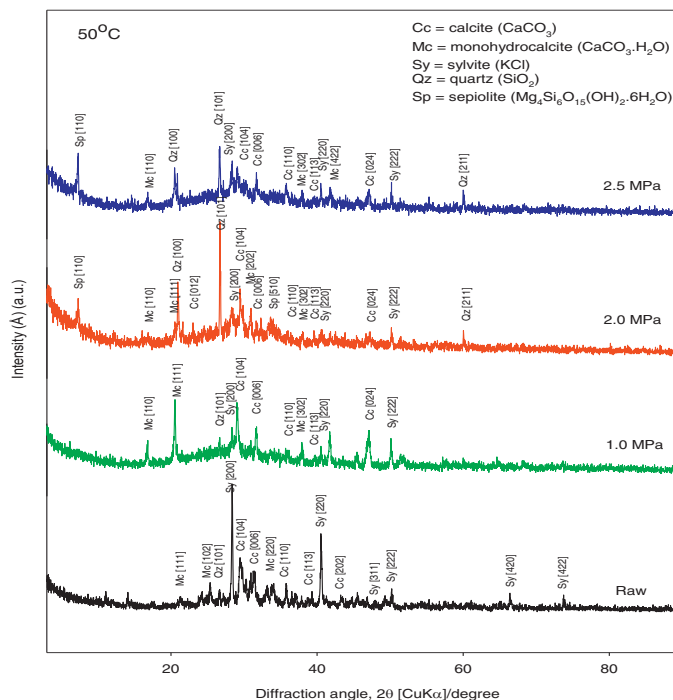


Fig. 2. The XRD patterns derived from raw K-rich ash and solid products at selected 50 °C and treated CO₂ pressure

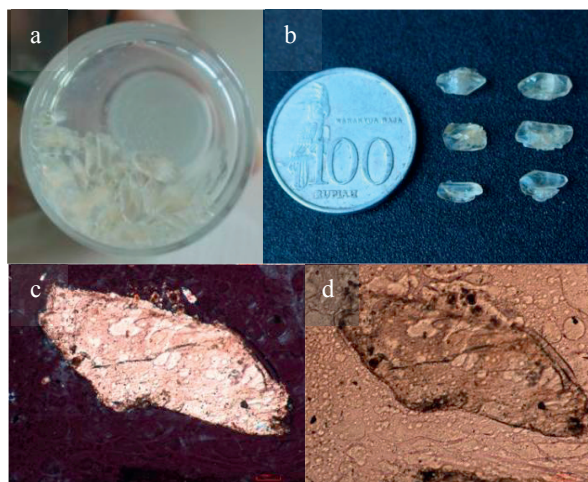


Fig. 3. (a) the photograph of precipitated and crystallized products in the liquid products at selected 100 °C and treated 2.5 MPa CO₂ pressure; (b) rhombohedral calcite shape; (c) calcite under cross—polarized light petrography (d) calcite under plane—polarized light petrography

The photograph and petrographical image of solid product identical with calcite crystal. The photograph images of solid product (Fig. 3) commonly showing appearance of transparent–translucent calcite crystal with rhombohedral shape which belongs to hexagonal crystal system. The petrographical image under plane–polarized light showing

colorless mineral, with euhedra shape and very high relief. Whereas under cross-polarized light showing high order birefringence colors and simple twinning.

The comparison of XRD spectra of the K-rich ash material and the solid product (Fig. 2), pH, EC and TIC analysis in the solutions and thermodynamic calculations suggest a simple reaction mechanism for CO₂ mineral sequestration by K-rich ash in two successive steps: first, the irreversible hydration of calcium oxide or lime:



second, the spontaneous carbonation of calcium hydroxide suspension:



It was recorded that this global reaction takes place at alkaline pH because the dispersion of the K-rich ash in pure water at atmospheric conditions for solid to liquid ratios for about 20 wt% increases the solution pH up to about 8.7 units (at 100 °C). The aqueous carbonation of Ca(OH)₂ described by the global reaction (3) is an exothermic process¹³ that concerns simultaneously the dissolution of Ca(OH)₂,



and the dissociation of aqueous CO₂,



these processes produce a fast supersaturation (*S_I*) of solution with respect to calcite,

$$S_I = (\text{Ca}^{2+})(\text{CO}_3^{2-}) / K_{sp} > 1 \quad (5)$$

where (Ca²⁺) and (CO₃²⁻) are the activities of calcium and carbonate ions in the solution, respectively, and *K_{sp}* is the thermodynamic solubility product of calcite. Then, the nucleation stage (formation of nuclei or critical cluster) takes place in the system,



Finally, the crystal growth occurs spontaneously until the equilibrium calcite and the solution is reached,



In the present study, the effects of K-rich ash, the CO₂ pressure, the reaction temperature and the reaction time are shown in Fig. 4. Amount of 250 g of ultra and high-purity water with electrical resistivity of 18.2 MΩ·cm at 25 °C and 50 g of K-rich ash were placed in a autoclave batch type reactor. The K-rich ash particles were immediately dispersed by mechanical stirring (200 rpm). The experiments were also carried out at room temperature (20 to 25) °C. When the dispersion temperature was reached, 1 MPa, 2MPa or 2.5 MPa of CO₂ was purged in the reactor (see Fig. 1). This was the initial pressure of CO₂ which was equal to the total initial pressure in the system. After CO₂ injection, the pressure drop was monitored as a function of time until CO₂ equilibrium pressure in the system (anisobaric system) in order to estimate separately the rate of CO₂ transfer in pure water and during carbonation process from the dispersion as also presented¹³.

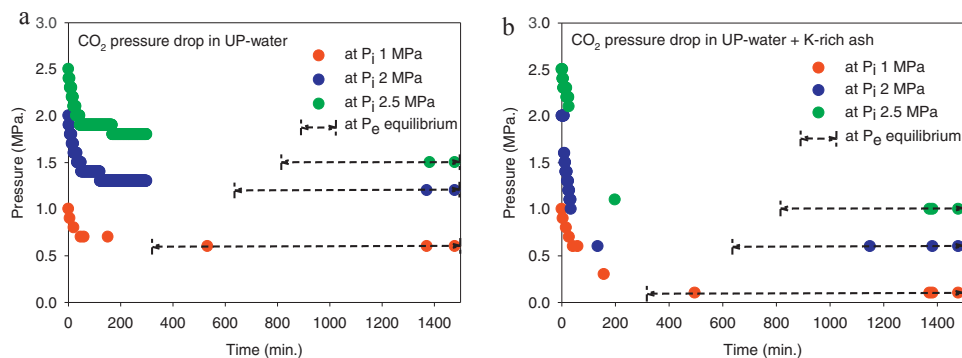


Fig. 4. (a) produced CO₂ pressure drop derived from ultra pure water (UP-water) at room temperature and treated CO₂ pressure; (b) produced CO₂ pressure drop derived from ultra pure water (UP-water) and raw K-rich ash at room temperature and treated CO₂ pressure

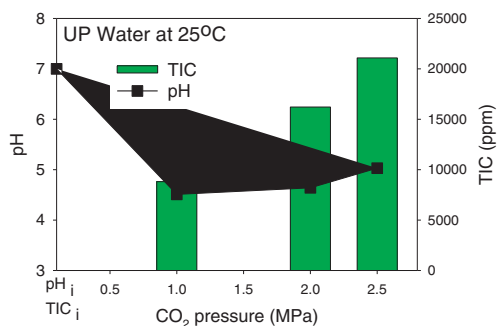


Fig. 5. Recorded pH and TIC of the sorption-dissociation of CO₂ in the UP-water at room temperature

Obviously, both the sorption-dissociation of CO₂ in the solution and hydrothermal carbonation process produce a global pressure drop in the system results to CO₂ mineral sequestration. In order to estimate the pressure drop produced by the total process of carbonation, two complementary systems were proposed for each experiment¹³. First, the pressure drop of ultra pure water (UP) related to the sorption-dissociation of CO₂ into pure water only was measured. Secondly, the pressure drop related to the sorption-dissociation of CO₂ in a K-rich ash solution was measured independently. In this second experiment, a concentration of about 20 wt% was chosen, that represented the average concentration after K-rich ash dispersion in water. Recorded pH and TIC of UP-water experiment is representing in Fig. 5 and mostly reaction takes place at acidic pH in a bicarbonate form (HCO₃⁻) of its sorption-dissociation of CO₂. These two experiments demonstrated that on the rate of sorption-dissociation of CO₂ of K-rich ash solution was faster than first water system because the monitored pressure drop in pure water was longer to reach the equilibrium pressure as shown in Fig. 4.

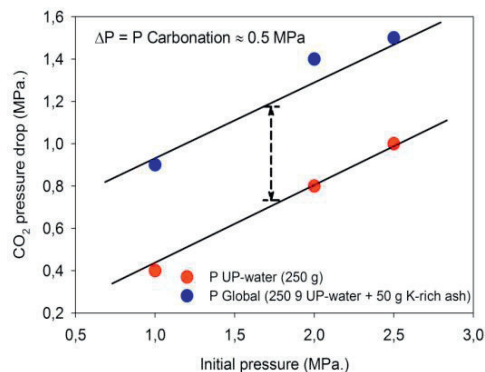


Fig. 6. Linear correlation between the pressure decrease at equilibrium and the initial pressure of CO₂ (from 1 MPa to 2.5 MPa)

A simplified method as describe in reference¹³ was developed to estimate the sequestered quantity of CO₂ by carbonate precipitation. Herein, the pressure drop produced by the carbonation process of K-rich ash and ultra pure water in the system was calculated by a simple pressure balance. Consequently, the pressure drop produced by the carbonation process of CaO (8.18 wt%) was calculated by a simple pressure balance:

$$P_{\text{carbonation pressure-drop}} = P_{\text{global pressure-drop}} - P_{\text{water pressure-drop}} \quad (8)$$

The carbonation pressure drop ($P_{\text{carbonation pressure-drop}}$) was close to 0.5 MPa and it was independent on the initial pressure of CO₂ (1 MPa, 2 MPa and 2.5 MPa) after 24 h of solid-liquid interaction (Fig. 4 and 6). For these experiments, water to fly-ash ratio equal to 10 (w/w) and 30 °C of reaction temperature were used. Systematically, the pressure drop was monitored with the time. These kinetic data showed that the CO₂ equilibrium pressure was reached after about 2 h of K-rich ash-fluid interaction. In contrast, the CO₂ equilibrium pressure in pure water was reached after about 3 h. This means that the carbonation process enhances the rate of CO₂ transfer in the system. Considering that CO₂ is an ideal gas, the quantity of CO₂ consumed by the carbonation process can be calculated as follows:

$$n_{\text{CO}_2} = P_{\text{carbonation pressure-drop}} V / RT \quad (9)$$

where, the V is the reactor volume occupied with gas (0.5 L), T is the temperature of reaction (≈ 303 °K) and R is the gas constant (0.08314472 L bar/°K mol). Using the calculated value $P_{\text{carbonation pressure-drop}} = 0.5$ MPa, as calculated that 0.0925 mol of CO₂ were consumed by the carbonation process. Taking into account reactions (2) and (3) and the fact that the K-rich ash contains 8.178 wt% of lime (CaO), the carbonation efficiency CE can be calculated by the following expression:

$$CE = n_{\text{CO}_2} M_{\text{CO}_2} / (w_{\text{CaO}} / M_{\text{CaO}}) M_{\text{CO}_2} \times 100 \quad (10)$$

where, n_{CO_2} is the mol number of consumed CO₂, calculated by Eq. (9) (0.0925 mol), M_{CO_2} is the molar mass of CO₂ (44.01 g/mol), w_{CaO} is the starting mass of CaO in the reactor (4.1 g) and M_{CaO} is the molar mass of CaO (56.077 g/mol). The carbonation efficiency was then calculated to 25.36 % after 24 h of solid-fluid interactions at 25 °C.

The monitoring of the pressure drop for any controlled system under ideal gas conditions allows the kinetic modelling of CO₂ transfer after gas injection in an aqueous solution or in a solid-liquid system (K-rich ash-water dispersion for this study) as described in reference¹³. This can be done using a simple correlation function, $n_{\text{total CO}_2} = f(t)$, where $n_{\text{total CO}_2}$ is the total mol quantity of CO₂ to be sequestered in UP-water or in the K-rich ash-water dispersion and t is the time after gas injection. For this case, the best fit (attested by a correlation factor close to 1) of the experimental-calculated data was achieved when using a pseudo-second-order kinetic model according to the following expression:

$$d n_{\text{total CO}_2, t} / dt = k_s (n_{\text{total CO}_2, \text{max}} - n_{\text{total CO}_2, t})^2 \quad (11)$$

where k_s is the rate constant of sequestered CO₂ (1/mol s) for a given initial pressure of CO₂ in the system, $n_{\text{total CO}_2, \text{max}}$ is the maximum sequestered quantity of carbon dioxide at equilibrium [mol], $n_{\text{total CO}_2, t}$ is the sequestered quantity of carbon dioxide at any time, t (mol).

The integrated form of Eq. (11) for the boundary conditions $t=0$ to $t=t$ and $n_{\text{total CO}_2, t} = 0$ to $n_{\text{total CO}_2, t} = n_{\text{total CO}_2, t}$ is represented by a hyperbolic equation:

$$n_{\text{total CO}_2, t} = n_{\text{total CO}_2, \text{max}} t / (1/k_s n_{\text{total CO}_2, \text{max}}) + t \quad (12)$$

In order to simplify the fitting of experimental-calculated data¹³, have defined the constant $t_{1/2} = k_s n_{\text{total CO}_2, \text{max}}$ has been defined. Physically, $t_{1/2}$ represents the time after which half of the maximum sequestered quantity of carbon

dioxide was reached and is called “half-sequestered CO₂ time”. It can be used to calculate the initial rate of CO₂ transfer, $v_{0,s}$ (mol/s).

$$v_{0,s} = n_{\text{total}} \text{CO}_{2,\text{max}} / t_{1/2} = k_s (n_{\text{total}} \text{CO}_{2,\text{max}})^2 \quad (13)$$

The parameters $t_{1/2}$ and $n_{\text{total}} \text{CO}_{2,\text{max}}$ were estimated by applying a non-linear regression using the least-squares method. The initial rates of CO₂ transfer in UP-water and in water-K-rich ash suspension were calculated using Eq. (13). These results demonstrated that the initial rate of CO₂ transfer was enhanced by carbonation process for our experiments. In addition, it's well known that the CO₂ solubility in UP-water increase with an increase of pressure. The present study showed that initial rate of CO₂ transfer in pure water also increases with pressure (from 1 MPa to 3 MPa) (Fig. 7).

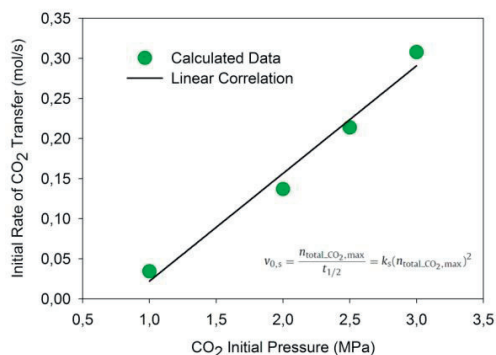


Fig. 7. linear increase of initial rate of CO₂ transfer with CO₂ initial pressure (from 1 MPa, 2 MPa, 2.5 MPa and 3 MPa)

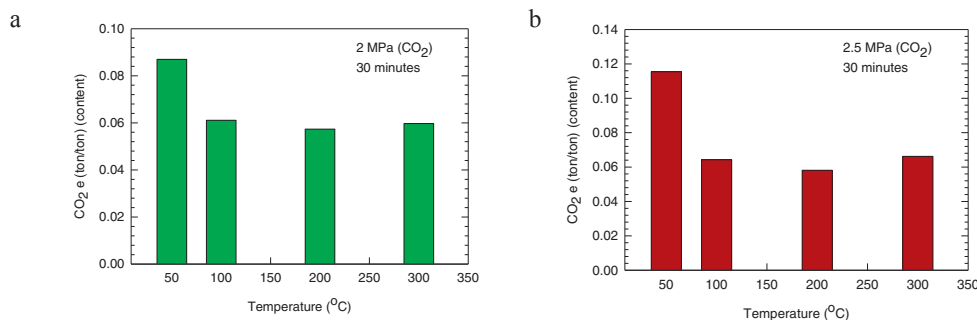


Fig. 8. (a) the amount of CO₂ content in hydrothermally treated solid product of K-rich ash at 2 MPa CO₂ pressure; (b) the amount of CO₂ content in hydrothermally treated solid product of K-rich ash at 2.5 MPa CO₂ pressure

Fig. 8. explained the amount of CO₂ content in hydrothermally treated solid product of K-rich ash. These indicated that as increasing treated temperature results in decreasing of CO₂ content in hydrothermally treated solid product. As increasing of treated pressurized CO₂ gas results in increasing of CO₂ content in hydrothermally treated solid product. At 50 °C, both treatment at 2.0 MPa and 2.5 Mpa of pressurized CO₂ gas has the maximum CO₂ content of solid products at 0.087 ton · ton⁻¹ and 0.115 ton · ton⁻¹ following the hydrothermal carbonation respectively.

4. Conclusion

In this research and study, hydrothermal carbonation of raw K-rich ash was evaluated at temperatures ranging from 50 °C to 300 °C at purged CO₂ gas of 2.0 Mpa and 2.5 MPa, a maximum final pressure of 8.5 MPa and a residence time of 30 min. Raw K-rich ash has potentially for the CO₂ sequestered and captured material. The

sequestered capacity of the K-rich ash depends on the treated temperature and purged CO₂ gas. Also, it was to demonstrate the feasibility to use K-rich ash to sequester CO₂ under mineral form via CaO carbonation. The results revealed a significant significant CaO—CaCO₃ chemical transformation by using a simplified pressure-mass balance method. In addition, the kinetic data demonstrated that the initial rate of CO₂ transfer was enhanced by carbonation process in our experiments.

Acknowledgment

The authors gratefully acknowledge the contributions of PTP Nusantara XIII (Persero) Pontianak, West Kalimantan, Indonesia for serving us the sample and assistances of Center for Wetlands People and Biodiversity-Tanjungpura University, Indonesia for serving us during the field research and experiment and contribution of intern students from Universitas Pendidikan Indonesia (UPI). The authors also gratefully acknowledge the contribution of the Laboratory of Mineral Processing and Recycling-Kyushu University Japan and Laboratory of Mineral and Energy-Research Centre for Geotechnology LIPI for providing equipments and analytical instruments. Financial support was provided by an Indonesia Toray Science Foundation (ITSF) and partly Research Project of Prioritas Nasional (PN-9) Penelitian Geoteknologi Perubahan Iklim (National Priority (NP-9) Geotechnology Research on Climate Change).

References

1. British Petrol (BP). *BP statistical review of world energy*. 2009.
2. Page SE, Siebert F, Rieley JO, Boehm H-DV, Jaya A, Limin S. The amount of carbon released from peat and forest fires in Indonesia during 1997. *Nature* 2002;420:61–65.
3. Bachu S. Sequestration of CO₂ in geological media: criteria and approach for site selection in response to climate change. *Energy Convers Manage* 2000;41:953–970.
4. Bachu S. Sequestration of CO₂ in geological media in response to climate change: road map for site selection using the transform of the geological space into the CO₂ phase space. *Energy Convers Manage* 2002;43:87–102.
5. Bachu S, Adams JJ. Sequestration of CO₂ in geological media in response to climate change: capacity of deep saline aquifers to sequester CO₂ in solution. *Energy Convers Manage* 2003;44:3:151–175.
6. Friedmann SJ. Geological carbon dioxide sequestration. *Elements* 2007;3:179–184.
7. Kharaka YK, Cole DR, Hovorka SD, Gunter WD, Knauss KG, Friefeld BM. Gas–water–rock interactions in Frio formation following CO₂ injection: implications for the storage of greenhouse gases in sedimentary basins. *Geology* 2006;34:577–580.
8. Seifritz W. CO₂ disposal by means of silicates. *Nature* 1990;345:486.
9. Lackner KS, Wendt CH, Butt DP, Joyce EL, Sharp DH. Carbon dioxide disposal in carbonate minerals. *Energy* 1995;20(11):1 153–1 170.
10. Soong Y, Fauth DL, Howard BH, et al. CO₂ sequestration with brine solution and fly-ashes. *Energy Convers Manage* 2006;47:1 676–1 685.
11. Huijgen WJJ, Witkamp GJ, Comans RNJ. Mechanisms of aqueous wollastonite carbonation as a possible CO₂ sequestration process. *Chem Eng Sci* 2006;61:4 242–4 251.
12. Huijgen WJJ, Comans RNJ, Witkamp GJ. Cost evaluation of CO₂ sequestration by aqueous mineral carbonation. *Energy Convers Manage* 2007;48:1 923–1 933.
13. Montes-Hernandez G, Perez-Lopez R, Renard F, Nieto JM, Charlet L. Mineral sequestration of CO₂ by aqueous carbonation of coal combustion fly-ash. *J Hazard Mater* 2009;161:1 347–1 354.
14. Othman MR, Martunus, Zakaria R, Fernando WJN. Strategic planning on carbon capture from coal fired plants in Malaysia and Indonesia: a review. *Energy Policy* 2009;37:1 718–1 735.
15. Yantovski E, Gorski J, Smyth B, Elshof J-ten. Zero-emission fuel-fired power plants with ion transport membrane. *Energy* 2004;29:2 077–2 088.
16. UN (United Nations). *Implementation of the CDM in Asia and the Pacific: issues, challenges and opportunities*. New York; 2003a.
17. Mursito AT, Hirajima T, Sasaki K. Upgrading and dewatering of raw tropical peat by hydrothermal treatment. *Fuel* 2010;89:635–641.
18. Mursito AT, Hirajima T, Sasaki K. Alkaline hydrothermal de-ashing and desulfurization of low quality coal and its application to hydrogen-rich gas generation. *Energy Convers Manage* 2011;52:762–769.
19. Mursito AT, Widodo, Yulianti A, et al. Hydrothermal Synthesis of Recycled K-Rich Ash Obtained from Empty Fruit Bunch and Its Application for CO₂ Capture and Mineral Carbonation. In: Dwianto W, Suprapedi, Subiyanto B, et al. editors. *Proceedings of the 2nd International Symposium for Sustainable Humanosphere*; 2012 August 29; Bandung Indonesia; LAPAN; 2012:87–92.
20. Farmer VC. *The infrared spectra of minerals*. London: Mineralogical Society Monograph 1974.
21. Velde B, Martinez G. Effect of pressure on OH-stretching frequencies in kaolinite and ordered aluminous serpentine. *Am Mineral* 1981;66:196–200.